SELECTED TOPICS ON THE ACTIVE CONTROL OF HELICOPTER AEROMECHANICAL AND VIBRATION PROBLEMS

Peretz P. Friedmann
Mechanical, Aerospace and Nuclear Engineering Department
University of California
Los Angeles, CA 90024

ABSTRACT

This paper describes in a concise manner three selected topics on the active control of helicopter aeromechanical and vibration problems. The three topics are: (1) The active control of helicopter air-resonance using an LQG/LTR approach; (2) Simulation of higher harmonic control (HHC) applied to a four bladed hingeless helicopter rotor in forward flight; and (3) Vibration suppression in forward flight on a hingeless helicopter rotor using an actively controlled partial span trailing edge flap, mounted on the blade. Only a few selected illustrative results are presented. The results obtained clearly indicate that the partial span actively controlled flap has considerable potential for vibration reduction in helicopter rotors.

NOMENCLATURE

$[A(\psi)]$	system dynamic matrix
$[B(\bar{\psi})]$	control distribution matrix
$[C]$	output matrix
C_W	helicopter weight coefficient, $C_W = W/(\pi R^4 \rho_a \Omega^2)$
J	quadratic cost function
$[K(s)]$	compensator matrix
$[K_c]$	feedback gains
$[K_f]$	filter gains from solution of Riccati equations

M_F	fuselage mass, nondimensional
M_{HS}	control surface hinge moment
N_b	number of blades
P_{IBC}	power required to implement conventional IBC
P_{cs}	power required to implement control based on actively controlled flap
R	rotor radius
$[T]$	HHC transfer matrix
$\{u\}$	control input vector
$[W_\delta]$	diagonal weighting matrix on actively controlled flap deflection angles
W	helicopter weight
$[W_{\Delta\delta}]$	diagonal weighting matrix on change in actively controlled flap deflection angles
$[W_Z]$	diagonal weighting matrix on vibrations
$[W_\theta]$	diagonal weighting matrix on control amplitudes
$\{x\}$	state variable vector
$\{Z(i)\}$	vector of vibration amplitudes
$\{Z_0\}$	vector of baseline vibrations

Greek Symbols

γ	Lock number
$\delta(\psi)$	control surface deflection angle
δ_{NC}, δ_{NS}	N/rev cosine and sine amplitudes of control input
θ_{IBC}	additional pitch inputs for conventional IBC
$\{\theta^*(i)\}$	optimal HHC input vector
$\{\theta(i)\}$	HHC input vector
$\{\Delta\theta(i)\}$	change in HHC input vector
θ_{pk}	pitch input to the k^{th} blade for air resonance suppression
θ_0	collective pitch angle
θ_{1s}, θ_{1c}	cyclic pitch components required for trim

$\Delta\theta_{1s}, \Delta\theta_{1c}$	sine and cosine control components introduced through a non-rotating swashplate
θ_{HH}	higher harmonic control angle in rotating frame
$\theta_{0s}, \theta_{cs}, \theta_{ss}$	amplitudes of HHC sine input in collective, longitudinal, and lateral control degrees of freedom
$\theta_{0c}, \theta_{cc}, \theta_{cs}$	amplitudes of HHC cosine input in collective, longitudinal and lateral degrees of freedom
μ	advance ratio
σ	blade solidity
ρ_a	air density
ψ	blade azimuth
ψ_k	k^{th} blade azimuth
$\omega_{F1}, \omega_{L1}, \omega_{T1}$	rotating first flap, lag and torsional blade frequencies nondimensionalized with respect to Ω
ω_{HH}	HHC frequency
Ω	rotor angular speed
$(\dot{})$	derivative with respect to ψ

INTRODUCTION

The use of active controls whereby the pitch of a helicopter rotor blade is modified by a control system so as to alleviate dynamic effects represents a typical aeroservoelastic problem. The level and scope of the research activity in this area have been increasing steadily during the last twenty years, and the body of related literature is quite substantial. A recent comprehensive survey article has described these topics with considerable detail (ref. 1).

The purpose of this paper is to present in a concise manner three selected topics on the active control of helicopter aeromechanical and vibration problems. The three topics described here are:

(1) The active control of helicopter air resonance using an LQG/LTR approach (refs. 2-5).

(2) Simulation of higher harmonic control (HHC) applied to a four bladed hingeless rotor in forward flight (refs. 6-8).

(3) Vibration suppression in forward flight on a hingeless helicopter rotor using an actively controlled, partial span flap, mounted on the blade (refs. 9 and 25).

It should be emphasized that only concise descriptions and selected results are presented here; the interested reader can find considerable additional material in refs. 1-9, and 25.

ACTIVE CONTROL OF HELICOPTER AIR RESONANCE

Air resonance is an aeromechanical instability experienced by a helicopter in hover or forward flight. It is caused by coupling between the blade lead-lag degree of freedom with fuselage pitch or roll. Air resonance is a fairly mild type of instability when compared to ground resonance (refs. 10-12).

Improved understanding of aeromechanical phenomena such as air resonance in hover and forward flight combined with advances in modern control technology offer the potential for practical active control of air resonance in hover and in forward flight. Previous studies (refs. 13-14) neglected the important effects of blade torsional flexibility, forward flight, and unsteady aerodynamics. Furthermore, for practical applications one has to demonstrate the ability of the control system to operate throughout a wide range of operating conditions encountered, while using a small number of measurements and control inputs. These problems were addressed in detail in a fundamental and innovative series of studies (refs. 2-5). These comprehensive studies demonstrated the feasibility of designing a simple active controller capable of suppressing air resonance throughout the complete range of operating conditions which may be encountered by a hingeless rotor helicopter.

The coupled rotor/fuselage model used in this study is shown in Fig. 1. The fuselage is assumed to be a rigid body with three translational degrees of freedom and two rotational degrees of freedom, namely pitch and roll. Yaw is ignored since its effect on the air resonance problem is known to be small. An offset hinged spring restrained blade model, shown in Fig. 2, is used to represent the hingeless blade. In this model, the blade elasticity is concentrated at a single point called the hinge offset point, and torsional springs are used to represent this flexibility. This assumption simplifies the equations of

motion, while retaining the essential features of the air resonance problem. The dynamic behavior of the rotor blade is represented by three degrees of freedom, which are flap, lag, and torsional motions. The aerodynamic loads of the rotor blades are calculated using a quasi-steady two dimensional potential flow strip theory. Compressibility and dynamic stall effects are neglected, although they could be important at high advance ratios. Unsteady aerodynamic effects, which are created by the time dependent wake shed by the airfoil as it undergoes arbitrary time dependent motion, are accounted for by using a dynamic inflow model. This model is described by a 3-state linear model forced by perturbations in the aerodynamic thrust, roll moment, and pitch moment at the rotor hub. The three states in these equations describe the behavior of the perturbations in the induced inflow through the rotor plane.

The equations of motion of the coupled rotor/fuselage system are complex and contain geometrically nonlinear terms due to moderate blade deflections in the aerodynamic, inertial, and structural forces. For this reason, the equations were derived and analytically linearized about the helicopter trim using a symbolic manipulation program (ref. 5). An ordering scheme was applied to the problem to further simplify the derivation. Despite the simplifications used, the mathematical model is quite substantial. The fuselage has 5 degrees of freedom; each blade has 3 degrees of freedom, thus the four bladed hingeless rotor is represented by 12 degrees of freedom; and there are three aerodynamic states associated with the dynamic inflow model. Thus the equations of motion are represented by 37 states.

The active control inputs to suppress the air resonance instability are introduced through a conventional swashplate; the pitch of the k^{th} rotor blade is given by the expression

$$\theta_{pk} = (\theta_0 + \Delta\theta_0) + (\theta_{1c} + \Delta\theta_{1c})\cos\psi_k + (\theta_{1s} + \Delta\theta_{1s})\sin\psi_k \qquad (1)$$

The terms with Δ are small and these represent the active control inputs, while those without Δ are the inputs necessary to trim the vehicle.

The stability of the system is determined through the linearization of the equations of motion about a blade equilibrium solution and the helicopter trim solution. The helicopter trim and equilibrium are extracted simultaneously using harmonic balance for a

straight and level flight condition. After linearization, a multiblade coordinate transformation is applied, which transforms the set of rotating blade degrees of freedom to a set of hub fixed non-rotating coordinates. The transformation is introduced in order to take advantage of the favorable properties of the non-rotating coordinate representation. The original system, before the transformation, has periodic coefficients with a fundamental frequency of 1/rev; however, the transformed system has coefficients with higher fundamental frequency. These higher frequency periodic terms have a reduced influence on the behavior of the system and can be ignored in some analyses at low advance ratios. In hover, the original system has periodic coefficients with a frequency of 1/rev, but the transformed system has constant coefficients. Two other properties of the model in hover are that the collective modes decouple from the sine and cosine modes of the system, and differential modes become uncontrollable. Thus, in hover, depending on what outputs and inputs are selected, the model may have uncontrollable and unobservable modes.

Once the multiblade coordinate transformation is carried out, the system is rewritten in first order form

$$\{\dot{x}\} = [A(\psi)]\{x\} + [B(\psi)]\{u\} \tag{2}$$

The system is constant coefficient in hover and becomes periodic as the forward flight speed is increased. Stability can be determined by using an eigenvalue analysis or by using Floquet theory for the periodic problem in forward flight (ref. 10). An approximate stability analysis in forward flight is also possible by performing an eigenvalue analysis on the constant coefficient portion of the system matrices in Eq. (2).

The study described in refs. 2-5 consisted of two stages. In the first stage (ref. 2) linear quadratic optimal control theory was used to design full state feedback controllers. It was found that the periodic terms in the model play only a small role for advance ratios below $\mu = 0.40$. However, the torsional degree of freedom and unsteady aerodynamics were found to be important. It was also determined that full state feedback was impractical and partial state feedback is unreliable.

Figure 3, taken from ref. 2, illustrates the effect of unsteady aerodynamics and periodic coefficients on the open loop system. The coupled rotor/fuselage configuration selected was a four bladed, soft-in-plane, hingeless rotor helicopter somewhat similar to the

MBB B0105 helicopter, in which certain parameters were modified, so as to induce an unstable air resonance mode, which manifests itself in the regressing lead-lag mode. Figure 3 depicts the damping in the lead-lag mode. The two sets of curves represent air resonance damping with quasi-steady aerodynamics and dynamic inflow, at various advance ratios. Dynamic inflow captures primarily the low frequency unsteady aerodynamic effect which is important for air resonance, and therefore this effect should be included in the controller design. It is also evident from the figure that the effect of periodic coefficients is relatively minor, thus controller design can be based on the constant coefficient approximation of the system represented by Eq. (2).

In the second stage of the research (refs. 3-5), a multivariable compensator was designed using two swashplate inputs and a single body roll rate measurement. The controller design is based on the LQG technique and the Loop Transfer Recovery Method (refs. 15-18). The controller is based on the optimal state estimator in conjunction with optimal feedback gains. A constant coefficient model is assumed, since the results shown in Fig. 3 as well as preliminary control studies (ref. 2) indicated that a periodic model was unnecessary. The compensator has the form (refs. 3-5).

$$[K(s)] = [K_c](S[I] - [A] + [B][K_c] + [K_f][C])^{-1}[K_f] \tag{3}$$

To introduce "robustness" into the controller the multivariable frequency domain design methods of refs. 15 and 16 were used. The representation of the model error is based on unstructured multiplicative uncertainty at the model output. Details on the design process can be found in refs. 3-5.

The controller design approach used was based on the selection of an operating point to design a constant gain controller, and used this controller throughout the operating range of the helicopter. The design point chosen is at hover ($\mu = 0$) with the nominal weight ($M_F = 32$), which is a point near the region of worst instability for the configuration. A single roll rate measurement of the fuselage and the sine and cosine swashplate inputs are chosen to control the instability.

In order to keep the compensator order low, a reduced model is formed and used in the design process. This reduction is accomplished by transforming the full system to block diagonal form and then removing the modes from the full model that are deemed

unnecessary to characterize the system dynamics in the frequency range of interest. An acceptable design model is one consisting of the body roll, body pitch, lead-lag progressing and the lead-lag regressing modes (refs. 3 and 5).

Typical results demonstrating the effectiveness of this controller are shown in Figs. 4 and 5. The open loop lead-lag regressing mode damping of the helicopter configuration throughout its flight regime is presented in Fig. 4. The horizontal axis is the advance ratio, while the vertical axis is the fuselage mass M_F nondimensionalized by the blade mass of 52 Kg. The figure indicates that the system experiences an air resonance instability throughout most of the flight regime. Marginal stability exists at an advance ratio greater than $\mu = 0.35$ and the point of deepest instability is at $M_F = 30$ and in the vicinity of hover. Figure 5 shows the same system after the controller, designed according to methodology discussed above, has been applied on the helicopter. From the figure it is clear that the lead-lag regressing mode is stable over the whole flight regime, and its stability is lowest in the neighborhood of $M_F = 23$ and $\mu = 0.11$. Time simulations were also conducted to check the controller and to verify that the periodic terms in the full model do not significantly alter the stability results. The time simulation also showed that the closed loop system could suppress angular roll rates as large as 6.5 deg/sec with less than two degrees of swashplate input.

However, it should be mentioned that these studies (refs. 2-5) did not consider interactions between the controller for air resonance suppression and the flight mechanics of the complete helicopter. Therefore, possible interactions between active control systems aimed at air or ground resonance and the conventional stability augmentation system (SAS) present on all helicopters have to be carefully studied in the future to avoid potentially negative interactions from a handling qualities point of view.

AEROELASTIC SIMULATION OF HIGHER HARMONIC CONTROL

One of the most important topics, from a practical point of view, is vibration reduction in forward flight using higher harmonic control (HHC), applied through a conventional swashplate. This approach reduces vibration levels in the fuselage, or at the hub, by modifying the vibratory aerodynamic loads on the blades. Thus vibratory forces

and loads are modified, at their source, before they propagate into the airframe. This is in contrast to conventional means of vibration control which deals with the vibratory loads after they have been generated. Furthermore, it should be noted that this approach also has the potential for reducing vibration in the fuselage caused by rotor fuselage unsteady aerodynamic interference (ref. 1).

The majority of these HHC studies, either analytical or experimental (ref. 1), have been based on linear, quasistatic, frequency domain representations of the helicopter response to control. Least squares or Kalman filter type identification of helicopter control parameters has been used together with a minimum variance of quadratic performance function type controllers to determine the optimal control harmonics for vibration alleviation. A detailed description of the control algorithm used in these studies can be found in refs. 6, 8, 19-21. In these studies the general HHC input is expressed as

$$\begin{aligned}\theta_{HH} = &[\theta_{0S}\sin\bar{\omega}_{HH}\psi + \theta_{0C}\cos\bar{\omega}_{HH}\psi] \\ &+ [\theta_{CS}\sin\bar{\omega}_{HH}\psi + \theta_{CC}\cos\bar{\omega}_{HH}\psi]\cos\psi \\ &+ [\theta_{SS}\sin\bar{\omega}_{HH}\psi + \theta_{SC}\cos\bar{\omega}_{HH}\psi]\sin\psi\end{aligned} \tag{4}$$

where $\theta_{0C}, \theta_{0S}, \theta_{CS}, \theta_{CC}, \theta_{SS}$, and θ_{SC} are independent of ψ.

Minimum variance controllers are obtained by minimization of the cost functional

$$J = E(\{Z(i)\}^T[W_Z]\{Z(i)\} + \{\theta(i)\}^T[W_\theta(i)]\{\theta(i)\} + \{\Delta\theta(i)\}^T[W_{\Delta\theta}]\{\Delta\theta(i)\}) \tag{5}$$

Typically $\{Z\}, \{\theta\}$, and $\{\Delta\theta\}$ consist of the sine and cosine components of N/rev. vibrations and HHC inputs. The weightings of each of the parameters may be changed to make a particular component more or less important than the other components.

The minimum variance controllers are obtained by taking the partial derivative of J with respect to $\{\theta(i)\}$

$$\frac{\partial J}{\partial\{\theta(i)\}} = 0 \tag{6}$$

the resulting set of equations may be solved for the optimal HHC input denoted by $\{\theta^*(i)\}$.

The form of the final algorithm will depend on whether the global or local system model is used and whether a deterministic or cautious controller is desired.

The global model of helicopter response to HHC is based on assuming linearity over the entire range of control application:

$$\{Z(i+1)\} = \{Z_0\} + [T]\{\theta(i)\} \tag{7}$$

The vibration vector $\{Z\}$ at step i + 1 is equal to the baseline uncontrolled vibration level $\{Z_0\}$ plus the product of the transfer matrix $[T]$ and the control vector $\{\theta\}$ at step i. This implies that $[T]$, which is the transfer matrix relating HHC inputs to vibration outputs, is independent of $\{\theta(i)\}$.

The local model of helicopter response to HHC is a linearization of the response about the response to the current value of the control vector:

$$\{Z(i+1)\} = \{Z(i)\} + [T](\{\theta(i+1)\} - \{\theta(i)\}) \tag{8}$$

or

$$\{\Delta Z(i+1)\} = [T]\{\Delta\theta(i+1)\} \tag{9}$$

which implies that the transfer matrix $[T]$ varies with the input $\{\theta\}$.

Each of these two algorithms has two versions, deterministic and cautious; this depends on the assumptions made on the noise characteristics for each row of the $\{Z_0\}$ and $[T]$ matrices.

Another ingredient in this algorithm is associated with identification. In applying HHC algorithms to vibration reduction, it is assumed that the HHC inputs $\{\theta(i)\}$ are known without error. Based on the measurements, different parameters may be identified. For the local model only the transfer matrix $[T]$ is identified. For the global model the transfer matrix $[T]$ and the baseline vibration vector $\{Z_0\}$ are identified. The general discrete Kalman filter is frequently used in the identification process (refs. 19-21).

Recently a comprehensive aeroelastic simulation capability has been developed (refs. 6-8) and used to study a number of fundamental issues in higher harmonic control. The analysis is based on a coupled flap-lag-torsional blade model in forward flight, with time domain unsteady aerodynamics and completely coupled aeroelastic response and trim analysis. The response analysis is based on three flap, two lag and the fundamental torsional mode. The four bladed hingeless rotor is assumed to be attached to a fixed, rigid fuselage; thus only hub shears and moments are simulated analytically. The higher harmonic control input is represented by Eq. (4). A deterministic and cautious minimum variance controller was programmed into algorithms, one for local and one for global HHC

models (refs. 6-8, 21).

The typical hingeless rotor blade considered in refs. 6-8 is shown in Fig. 6. Using this model various aspects of the HHC implementation on a soft-in-plane hingeless rotor were carefully studied. A few useful results and conclusions in these studies are briefly summarized below.

An interesting test of the ability of the controllers to adapt to changing flight conditions was performed by introducing a step change in advance ratio from $\mu = 0.30$ and $\mu = 0.35$. Results for a soft-in-plane hingeless rotor are shown in Fig. 7. A comparison of the three hub shear components and their values for the local and global controllers are shown. It is evident that the global controller has been more successful in reducing shears. Comparison of the effectiveness of the HHC to reduce vibration levels in a four bladed hingeless rotor and an equivalent four bladed articulated rotor was also conducted (ref. 8) and it was found that much larger HHC angles were required to reduce shears for the hingeless rotor. Careful comparisons of the power requirements needed for application of HHC to these two rotor configurations were also conducted, and it was found that the hingeless rotor required substantially more power.

Blade root loads and pitch link loads were also increased substantially when HHC was applied to the hingeless rotor. The conclusions imply that vibration reduction in the hingeless rotor using HHC could be more difficult to implement than in articulated rotors.

The effect of HHC on aeroelastic stability margins was also studied in ref. 6 and it was found that overall aeroelastic stability margins were not significantly degraded by application of HHC to either the articulated or the hingeless rotor configurations.

In another study (ref. 22) an important and closely related question was examined; namely, is vibration reduction at the hub equivalent to vibration reduction at various locations on a flexible fuselage when using HHC? Most analytical studies (refs. 6-8, 19-21) were based on the assumption that the fuselage is rigid and vibration reduction at the hub was assumed to be equivalent to vibration reduction at various fuselage locations. The fundamental study described in ref. 22 was based on a somewhat idealized nonlinear coupled rotor/flexible fuselage analysis capable of modeling the system shown in Fig. 8. It was found that conventional HHC inputs through a conventional swashplate, aimed at hub

shear reduction, cause an increase in the fuselage acceleration and vice versa. Furthermore it was found that for simultaneous reduction of both hub shears and fuselage accelerations, a pitch input consisting of a combination of two higher harmonic components having different frequencies was needed. However this input could not be introduced through a conventional swashplate, and it could only be implemented in the rotating reference frame. This study has also produced a new insight on the vibration reduction in coupled rotor/flexible fuselage systems by examining the sensitivity of hub shears to the frequency and amplitude of the open loop blade pitch input signals introduced in the rotating reference frame. The role of fuselage flexibility for this class of problems was also determined in ref. 22.

VIBRATION REDUCTION IN HELICOPTER ROTORS USING AN ACTIVELY CONTROLLED FLAP LOCATED ON THE BLADE

Recently a (ref. 9) detailed feasibility study was conducted to examine the potential for vibration reduction in hingeless (or bearingless) helicopter rotors by using an actively controlled flap located on the blade. Recall that comparative studies of vibration reduction in forward flight using HHC were conducted for similar articulated and hingeless rotors in refs. 6 and 8. For both configurations substantial vibration reduction was achieved with HHC angles under 3 degrees. However, a comparison of power requirements revealed that the power required to implement HHC on hingeless rotor blades is significantly higher than for equivalent articulated rotor blades. These higher power requirements appear to be associated with the need to drive harmonically the fairly large and coupled structural dynamic system represented by the hingeless blade.

This provided the motivation for exploring an alternative concept where the tailoring of the aerodynamic loads on the blade, for vibration reduction in forward flight, is accomplished through the active control of an aerodynamic surface located on the blade, similar to the partial span flap shown in Fig. 9. It was postulated that such a device would produce substantial reduction in power requirements when compared with HHC or conventional individual blade control (IBC) which require the introduction of cyclic pitch changes for the whole blade. Furthermore, such an actively controlled flap can be operated by a control loop which is separate from the primary control system; thus it will have no

influence on vehicle airworthiness, because it is not part of the primary control system of the vehicle and it will enable one to retain the conventional swashplate for flight control purposes. It should also be mentioned that this concept is not new. Almost twenty years ago Lemnios and Smith (ref. 23) used a servo flap in the context of their research on the controllable twist rotor (CTR). Using a combination of collective and cyclically varying twist distribution on the blade they demonstrated a considerable increase in performance and a 30% decrease in blade bending amplitudes.

The use of an actively controlled aerodynamic surface on each blade to reduce vibrations in forward flight falls into the category of IBC since each aerodynamic surface is individually controlled in the rotating reference frame. Such a configuration has the potential for reducing vibrations, requires less power, and retains the versatility of conventional IBC, without requiring the replacement of the conventional swashplate by a more complex mechanical system.

In the first stage of the feasibility study (ref. 9) a simple blade model consisting of an offset-hinged spring restrained blade with coupled flap, lead-lag and torsional dynamics was selected. This model was similar to that shown in Fig. 2, except that a partial span flap, shown in Fig. 9, has been added to the blade model. This partial span is used to introduce the appropriate control inputs for vibration reduction. The control surface deflection for the k^{th} blade is represented by a sum of harmonic input signals, in the rotating reference frame, having frequencies which are integer multiples of the rotor angular frequency, but greater than the 1/rev frequency needed for vehicle trim, i.e.,

$$\delta(\psi_k) = \sum_{N=2}^{N_{c\ max}} [\delta_{NC} \cos(N\psi_k) + \delta_{NS} \sin(N\psi_k)] \tag{10}$$

where $N_{c\ max}$ represents the largest integer multiple of the rotor frequency used in the harmonic control input. In this study $N_{c\ max}$ was set at 5.

The inertial loads obtained in ref. 9 included the inertial effect associated with the flap mounted on the blade. The aerodynamic loads on the blade were obtained from quasi-steady Greenberg theory and the reversed flow region was included; however compressibility and dynamic stall were neglected. The aerodynamic loads associated with the actively controlled flap were based on a quasi-steady version of Theodorsen's theory. The structural, inertial and aerodynamic loads on the isolated blade are obtained in explicit

form using MACSYMA (ref. 24). The blade equations of motion contain geometrically nonlinear terms due to moderate blade deflections. An ordering scheme is used to keep the explicit expressions to a manageable size (ref. 10). The resulting equations are solved for steady trimmed flight, assuming propulsive trim. The coupled trim/aeroelastic response solution for the blade is obtained using the harmonic balance method.

The control law is obtained by minimizing the objective function represented by Eq. (5). Both global and local controllers were studied. The global controller uses the following optimal control law

$$\{\delta^*(i)\} = [D]^{-1}(-[T]^T[W_Z]\{Z(i-1)\} + [W_{\Delta\delta}]\{\delta^*(i-1)\}) \tag{11}$$

where

$$[D] = ([T]^T[W_Z][T] + [W_\delta] + [W_{\Delta\delta}]) \tag{12}$$

The local controller is governed by

$$\{\delta^*(i) = [D]^{-1}(-[T]^T[W_Z]\{Z(i-1)\} + [W_{\Delta\delta}]\{\delta^*(i-1)\} + [T]^T[W_Z][T]\{\delta^*(i-1)\} \tag{13}$$

Additional algebraic details can be found in ref. 9. Equation (13) represents a closed loop controller where the control input of the i^{th} step is obtained by feedback of the measured response during the $(i-1)$ step $\{Z(i-1)\}$. The local controller converges quickly to the true optimal control law, usually in less than three steps.

Operating the control surface actuators needed to implement the control will of course require power from the helicopter powerplant. As a measure of the power required, the instantaneous power required to drive one control surface is averaged over one rotor revolution and multiplied by the number of blades (four in this case). The instantaneous power consists of the product of the instantaneous control surface hinge moment and the instantaneous angular velocity of the control surface. The net hinge moment consists of the sum of the inertial and aerodynamic moments about the hinge. Detailed expressions for the aerodynamic hinge moment are presented in ref. 9.

The average power required to implement the control using an active control surface on each blade is defined as:

$$P_{cs} = \sum_{k=1}^{N_b=4} \frac{1}{2\pi} \int_0^{2\pi} M_{Hcs}(\psi_k)\dot{\delta}(\psi_k)d\psi_k \tag{14}$$

Once the trim and response solution has been obtained, the rotor vibratory hub loads can be determined by summing the contribution from each blade of the rotor. The hub forces and hub moments of each blade are obtained in the rotating reference frame by integrating the distributed loads over the span of the blade. Subsequently the hub loads are transformed to the nonrotating hub fixed reference frame and the contribution from each blade in the rotor is summed over the number of blades. For a four bladed rotor the principal contribution to the rotor vibratory hub loads, after various algebraic and trigonometric manipulations are carried out, is the 4/rev vibratory component.

To illustrate the feasibility of this new approach to vibration reduction a number of active control studies were carried out on a soft-in-plane blade configuration at an advance ratio of $\mu = .30$. The pertinent details on this configuration can be found in ref. 9. The basic properties of this four bladed rotor are included here, so as to provide "physical feel" for the configuration considered. The fundamental rotating frequencies, for the baseline configuration, in flap, lag and torsion, respectively, were: $\omega_{F1} = 1.5$; $\omega_{L1} = 0.57$ and $\omega_{T1} = 2.5$. The thrust coefficient was $C_W = 0.005$, and $\sigma = 0.05$; $\gamma = 5.0$. The control surface was modeled as a 20% span, 1/4 chord partial span trailing edge flap centered about the 75% blade span station. The control input for minimizing the vibratory hub shears and moments consisted of a sum 2,3,4, and 5/rev harmonic input signal. The 3,4 and 5/rev input frequencies were selected because a 4/rev pitch input signal introduced in the nonrotating system through a conventional swashplate, which is frequently used in HHC studies on four bladed rotors, generates a signal consisting of 3,4 and 5/rev components in the rotating reference frame. The 2/rev component was added since it was found in ref. 22, that its role in vibration reduction is as significant as that of the other three components mentioned.

For the results presented here, only the vibration levels were penalized, i.e., $W_\delta = W_{\Delta\delta} = 0$. For this case the quadratic cost functional $J(i)$ consists of the weighted sum of the squares of the hub shears and hub moments, as evident from Eq. (5). The non-dimensional values of the baseline hub moments were an order of magnitude smaller than the hub shears. Therefore, the weights on the hub moments were set at 100 times the weights on the hub shears in order to ensure that an equivalent degree of vibration

reduction is achieved in all vibratory components.

Comparison of the vibration reduction obtained with the actively controlled flap, and individual blade control used on the same blade is presented in Figs. 10 and 11. Individual blade control (IBC) applied on the blade in the conventional sense implies that pitch input is provided at the root of the blade and the whole blade is oscillated in pitch, as a rigid body. When IBC is applied through an actively controlled flap, the pitch input is applied only to the small partial span flap. Figure 10 shows comparison of baseline hub shears and hub moments acting on blade, with those which are present when vibration reduction is implemented by the actively controlled flap. Figure 11 presents a similar comparison for the case of conventional IBC. In both figures results are presented for both the global and local controllers. These results indicate that similar degrees of vibration reduction are obtained for both the global and local approaches. It is also evident from Figs. 10 and 11 that the vertical hub shear was reduced to within 10% of its baseline value when using an actively controlled flap, compared to an average reduction to within 5% of its baseline value using conventional IBC. Very similar results were also obtained for the other five components of the vibratory hub loads. Overall, it appears that conventional IBC is slightly more effective in reducing the vibratory hub leads. However, the difference in the degree of vibration reduction achieved by the two control approaches is very small. A comparison of the optimal control input for vibration reduction using the individually controlled flap and conventional IBC for a blade having a fundamental torsional frequency of 2.5 is shown in Fig. 12. Examination of the optimal input signals reveals that somewhat larger control input amplitudes are required for vibration reduction when using the actively controlled flap compared to the angles required by conventional IBC. A maximum control surface deflection angle of 4 degrees is required compared to a maximum control angle of 0.9 degrees for conventional IBC. Numerous additional results, presented in ref. 9, indicate that larger control input amplitudes were required to achieve approximately the same degree of vibration reduction, when the torsional frequency of the blade is increased.

A comparison of the average power required (per revolution) for the implementation of the vibration reduction using the two control approaches is presented in Fig. 13. The power required for conventional IBC is defined as the average power needed to

drive the blade root pitch actuators during one revolution:

$$P_{IBC} = \sum_{k=1}^{N_b=4} \frac{1}{2\pi} \int_0^{2\pi} M_{x3}(\psi_k)\dot{\theta}_{IBC}(\psi_k)d\psi_k \tag{15}$$

where $\theta_{IBC}(\psi)$ represents the instantaneous additional IBC pitch input of the k^{th} blade and $M_{x3}(\psi)$ represents the instantaneous blade root feathering moment.

An examination of Fig. 13 reveals that substantially more power is required to implement vibration reduction using the conventional IBC approach than for vibration reduction based on the actively controlled flap. Vibration reduction using conventional IBC required about 800% more power at the lower blade torsional frequencies, and about 400% more power at the higher blade torsional frequencies. These higher power requirements appear to be associated with the need to drive harmonically the fairly large and coupled structural dynamic system represented by the entire blade, as opposed to the need to drive harmonically a relatively small aerodynamic control surface. It is also evident from this figure that as the torsional frequency of the blade increases, the power required to implement the control increases for both control approaches.

The results presented here together with the additional results presented in ref. 9 clearly indicate that the actively controlled flap is a feasible and very attractive concept, because it can produce the same vibration reduction as conventional IBC, with reasonable control angles and requires substantially less power (4 to 8 times less). Furthermore, it has the additional advantage of having no effect on the airworthiness when compared to conventional IBC.

Further studies on the practical implementation of an actively controlled flap to reduce vibrations in forward flight were presented in ref. 25. In this study, which represents a sequel to ref. 9, the offset hinged spring restrained blade model used previously was replaced by a completely flexible blade model. Control studies based upon the flexible blade model and the spring restrained blade model are compared. It was found that despite large increases in vibration levels due to the more realistic flexible blade model, vibration reduction could still be accomplished without excessive power expenditure or control angle inputs. A careful parametric study in which variations of torsional frequency, spanwise location of the control surface, and hinge moment correction factor was conducted. The results further reinforced the feasibility of this new approach to vibration

reduction. Numerous results obtained in this study can be found in ref. 25.

CONCLUDING REMARKS

During the last few years there has been a steady evolution of the application of active control technology to both stabilization of aeromechanical problems such as air and ground resonance as well as vibration reduction in forward flight.

Aeromechanical problems such as air and ground resonance are due to the low damping level associated with the inplane (lead-lag) degree of freedom and its coupling with fuselage roll. Thus this instability can be easily stabilized using active controls. However it is important to emphasize that the expense associated with using active control technology for aeromechanical stability augmentation can not be justified. Only vibration reduction in forward flight is sufficiently important so as to warrant the additional cost associated with active control technology. Once such a vibration reduction system has been installed it can also be used to stabilize aeromechanical problems. However, additional research is needed before the feasibility of stabilizing potential aeroelastic instabilities in rotors is verified.

Since modern rotor systems appear to move in the direction of hingeless and bearingless designs, the capability of conventional HHC or IBC may be limited by the need to oscillate the complete blade in pitch. In this context the actively controlled, partial span, trailing edge flap offers an attractive alternative which requires substantially less power and is fairly simple to implement. Therefore, this concept should be carefully studied using both simulation as well as wind tunnel tests.

ACKNOWLEDGEMENT

This research was funded in part by NASA Ames Research Center under grant NAG2-477; the useful comments of the grant monitor, Dr. S. Jacklin are gratefully acknowledged.

REFERENCES

1. Friedmann, Peretz, P.; Rotary-Wing Aeroservoelastic Problem. AIAA Paper No. 92-2107, Proceedings AIAA Dynamics Specialist Conference, April 16-17, 1992, Dallas, TX, pp. 248-272.

2. Takahashi, M.D.; and Friedmann, P.P.; Active Control of Helicopter Air Resonance in Hover and Forward Flight. AIAA Paper 88-2407, Proceedings of 29^{th} AIAA/ASME/ASCE/AHS Structures, Structural Dynamics and Materials Conference, April 18-20, Williamsburg, VA, pp. 1521-1532.

3. Takahashi, Marc, D.; Active Control of Helicopter Aeromechanical and Aeroelastic Instabilities. Ph.D. Dissertation, Mechanical, Aerospace and Nuclear Engineering Department, University of California, Los Angeles, June 1988.

4. Takahashi, M.D.; and Friedmann, P.P.; Design of a Simple Active Controller to Suppress Helicopter Air Resonance. Proceedings of the 44^{th} Annual Forum of the American Helicopter Society, Washington, DC, June 1988, pp. 305-316.

5. Takahashi, M.D.; and Friedmann, P.P.; Helicopter Air Resonance Modeling and Suppression Using Active Control. *AIAA Journal of Guidance, Control and Dynamics*, vol. 14, no. 6, Nov/Dec 1991, pp. 1294-1300.

6. Robinson, Lawson, H.; Aeroelastic Simulation of Higher Harmonic Control. Ph.D. Dissertation, Mechanical, Aerospace and Nuclear Engineering Department, University of California, Los Angeles, June 1989.

7. Robinson, L.H.; and Friedmann, P.P.; Analytical Simulation of Higher Harmonic Control Using a New Aeroelastic Model. AIAA Paper No. 89-1321, Proceedings of 30^{th} AIAA/ASME/ ASCE/AHS/ACS Structures, Structural Dynamics and Materials Conference, Mobile, AL, April 1989, Part III, pp. 1394-1406.

8. Robinson, L.H.; and Friedmann, P.P.; A Study of Fundamental Issues in Higher Harmonic Control Using Aeroelastic Simulation. *Journal of the American Helicopter Society*, vol. 36, no. 2, April 1991, pp. 32-43.

9. Millott, T.; and Friedmann, P.P.; Vibration Reduction in Helicopter Rotors Using an Active Control Surface Located on the Blade. AIAA Paper No. 92-2451, Proceedings of 33^{rd} AIAA/ASME/AHS/ACS Structures, Structural Dynamics and Materials Conference, April 13-15, 1992, Dallas, TX, pp. 1975-1988.

10. Friedmann, Peretz, P.; Formulation of Rotary-Wing Aeroelastic Stability and Response Problems, *Vertica*, vol. 7, no. 2, pp. 101-141, 1983.

11. Friedmann, Peretz, P.; Recent Trends in Rotary-Wing Aeroelasticity. *Vertica*, vol. 11,

no. 1/2, pp. 139-170, 1987.

12. Friedmann, Peretz, P.; Rotary-Wing Aeroelasticity with Application to VTOL Vehicles. AIAA Paper 90-1115, Proceedings of 31st AIAA/ASME/ASCE/AHS Structures, Structural Dynamics and Materials Conference, Long Beach, CA, April 2-4, 1990, pp. 1624-1670.
13. Straub, F.K.; and Warmbrodt, W.; The Use of Active Controls to Augment Rotor/Fuselage Stability. *Journal of the American Helicopter Society*, vol. 30, no. 3, pp. 13-22, 1985.
14. Straub, Friedrich, K.; Optimal Control of Helicopter Aeromechanical Stability. *Vertica*, vol. 11, no. 3, pp. 12-22, 1987.
15. Doyle, J.C.; and Stein, G.; Multivariable Feedback Design; Concepts for Classical/Modern Synthesis. *IEEE Transactions on Automatic Control*, vol. AC-32, no. 2, February 1987, pp. 105-114.
16. Stein, G.; The LQG/LTR Procedure for Multivariable Feedback Control Design. *IEEE Transactions on Automatic Control*, vol. AC-32, no. 2, February 1987, pp. 105-114.
17. Safonov, M.G.; Laub, A.J.; and Hartmann, G.L.; Feedback Properties of Multivariable Systems: The Role and Use of the Return Difference Matrix. *IEEE Transactions on Automatic Control*, vol. AC-26, no. 1, February 1981, pp. 47-65.
18. Madiwale, A.; and Williams, D.E.; Some Extensions of Loop Transfer Recovery. Proceedings of the American Control Conference, vol. 2, 1985, pp. 790-795.
19. Johnson, Wayne; Self-Tuning Regulators of Multicyclic Control of Helicopter Vibrations. NASA TP 1996, 1982.
20. Molusis, J.A.; Hammond, C.E.; and Cline, J.H.; A Unified Approach to the Optimal Design of Adaptive and Gain Scheduled Controllers to Achieve Minimum Helicopter Vibration. *Journal of the American Helicopter Society*, vol. 28, no. 2, pp. 9-18, April 1983.
21. Davis, Mark, W.; Refinement and Evaluation of Helicopter Real-Time Self-Adaptive Active Vibration Control Algorithms. NASA CR-3821, August 1984.
22. Papavassiliou, I,; Friedmann, P.P.; and Venkatesan, C.; Coupled Rotor/Fuselage Vibra-

tion Reduction Using Multiple Frequency Blade Pitch Control. Paper No. 91-76, Proceedings of Seventeenth European Rotorcraft Forum, September 24-26, 1991, Berlin, Germany, pp. 91-76.1 - 91-76.44.

23. Lemnios, A.Z.; Smith, A.F.; An Analytical Evaluation of the Controllable Twist Rotor Performance and Dynamic Behavior, Kaman Report R-794, 1972.

24. ___; MACSYMA: Reference Manual, Symbolics Inc., June 1986.

25. Millott, T.A.; Friedmann, P.P.; The Practical Implementation of an Actively Controlled Flap to Reduce Vibrations in Helicopter Rotors, Proceedings of 49^{th} Annual Forum of the American Helicopter Society, St. Louis, MO, May 19-21, 1993, pp. 1079-1092.

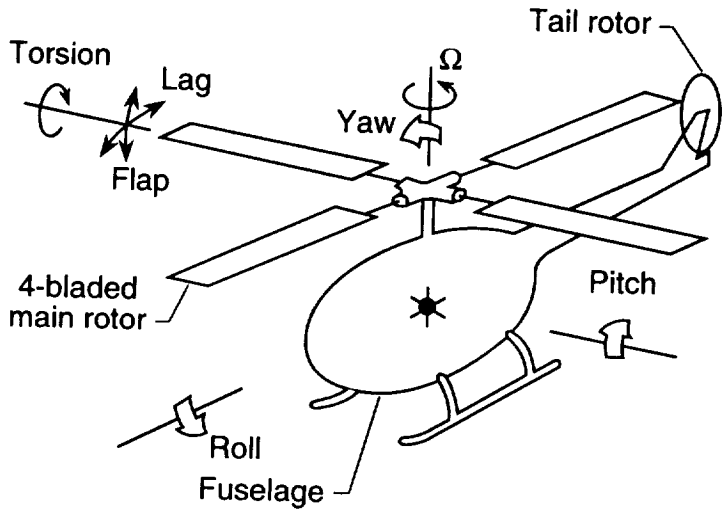

Fig. 1: Coupled rotor fuselage model

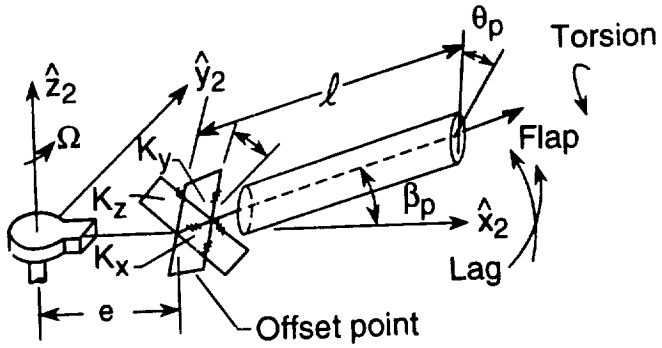

Fig. 2: Offset hinged spring restrained model for hingeless blade.

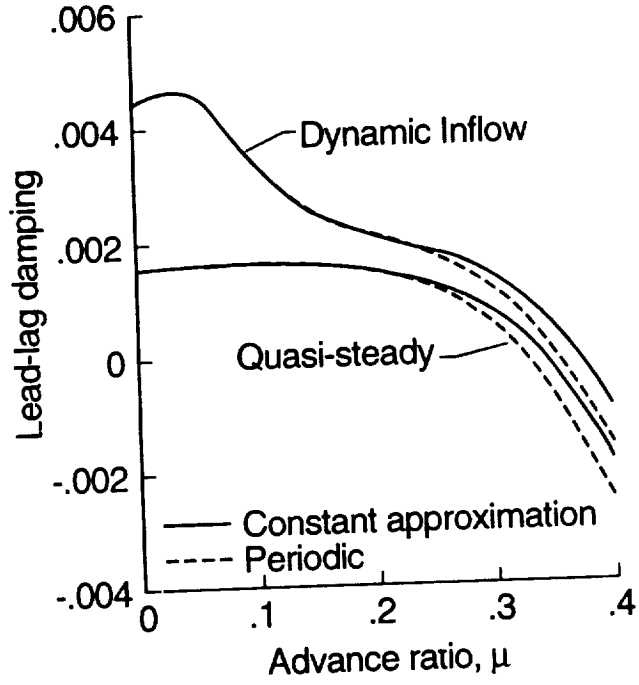

Fig. 3: Open loop lead-lag regressing damping of the nominal configurations with and without dynamic inflow.

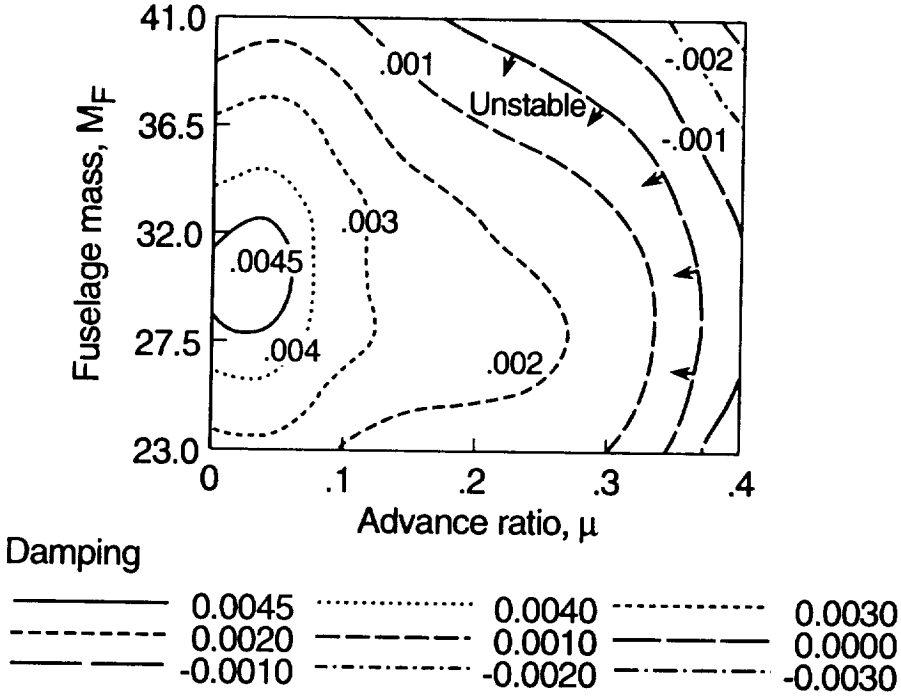

Fig. 4: Open loop lead-lag regressing mode damping at various weights and advance ratios

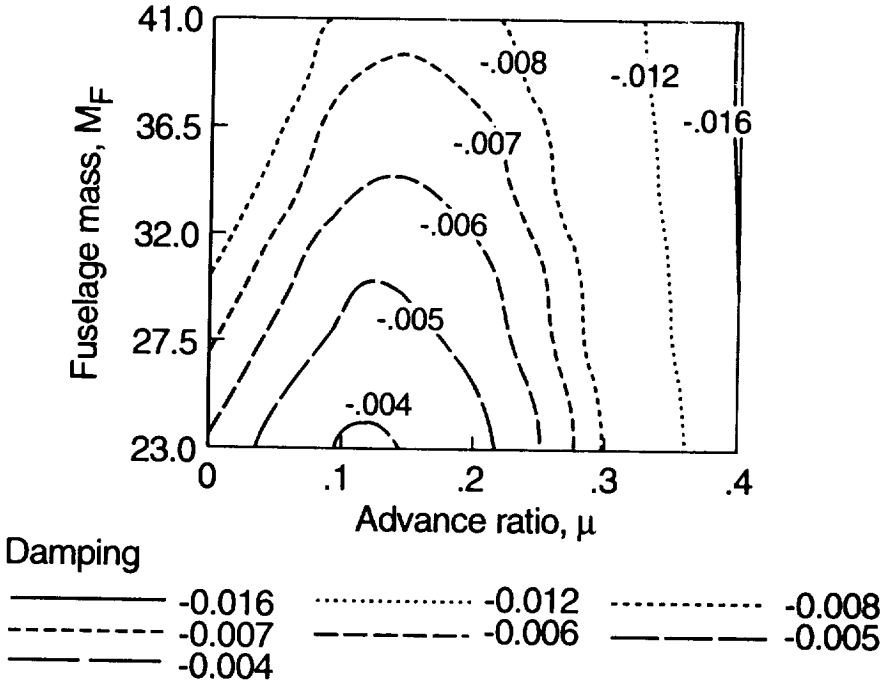

Fig. 5: Closed loop lead-lag regressing mode damping at various fuselage weights and advance ratios, using the active control

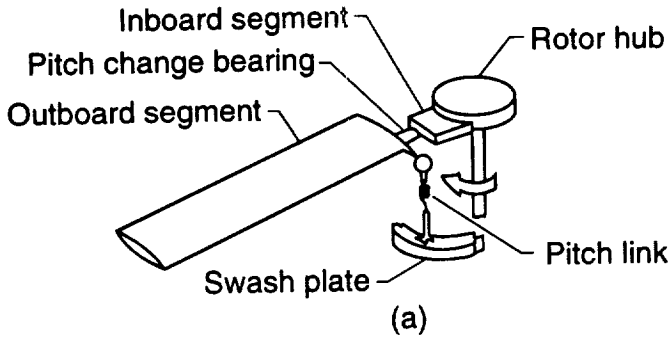

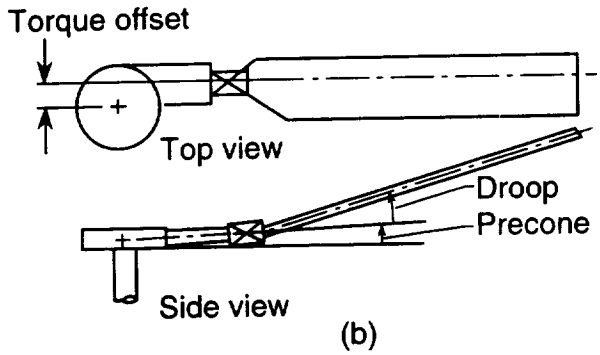

Fig. 6: Typical hingeless rotor blade geometry

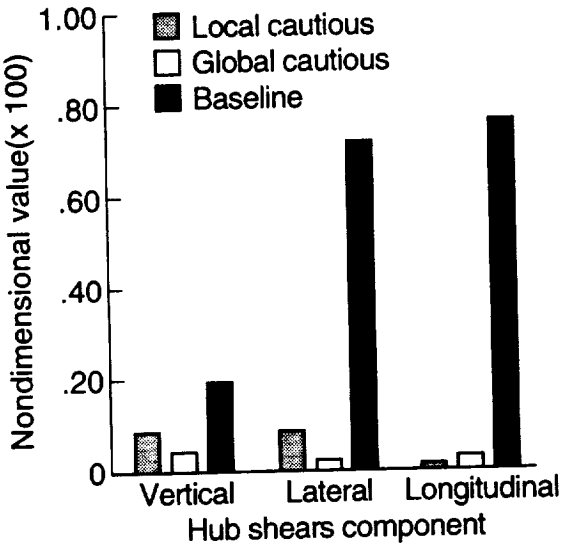

Fig. 7: Baseline shears for $\mu = 0.35$ and shear five iterations after a step change from $\mu = 0.30$ to $\mu = 0.35$, local and global controllers

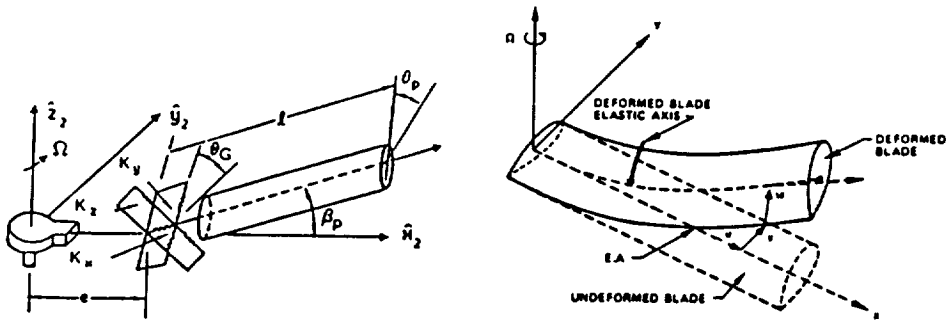

(a) Offset hinged spring restrained blade model

(b) Elastic blade model

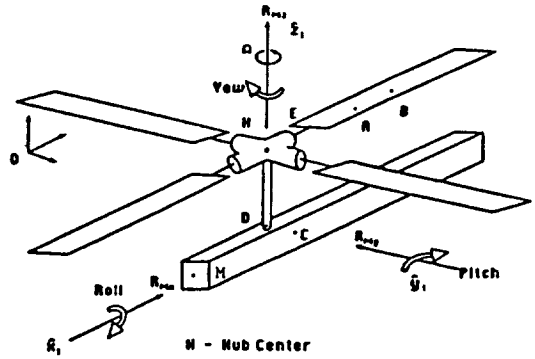

Fig. 8: Schematic representation of coupled rotor/flexible fuselage system, including two different types of blade models; (a) offset hinged blade and (b) fully elastic blade

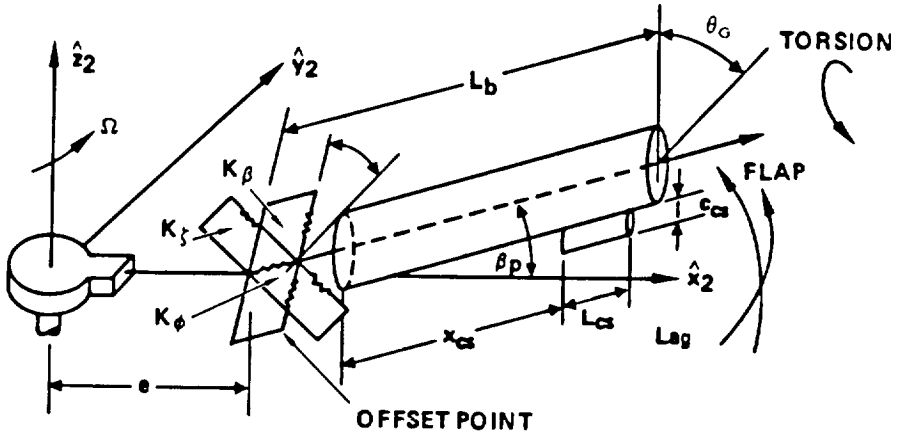

Fig. 9: Offset-hinged spring restrained hingeless rotor blade model with partial span flap

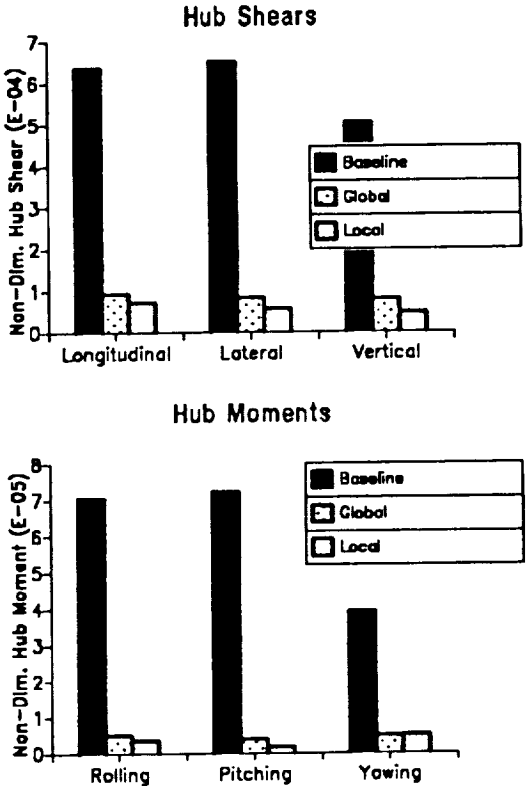

Fig. 10: Hub shears and moments for IBC using an actively controlled flap at a first rotating torsional frequency of 2.5/rev

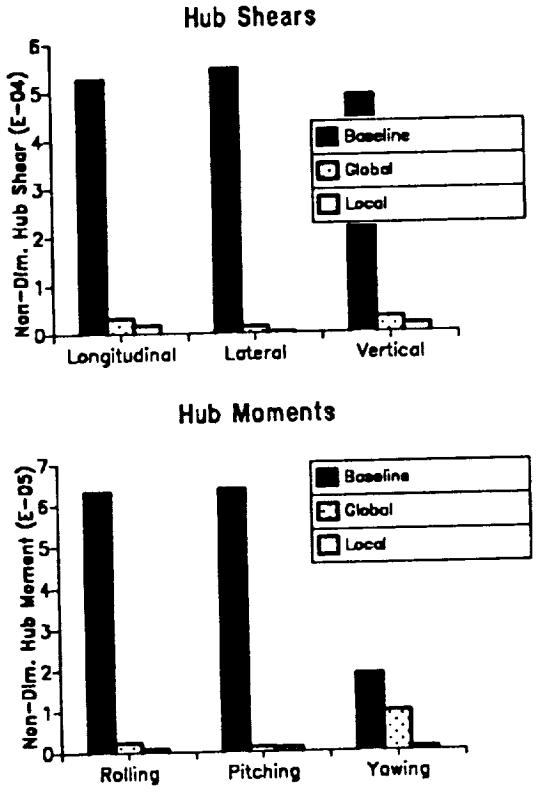

Fig. 11: Hub shears and moments for conventional IBC at a first rotating torsional frequency of 2.5/rev

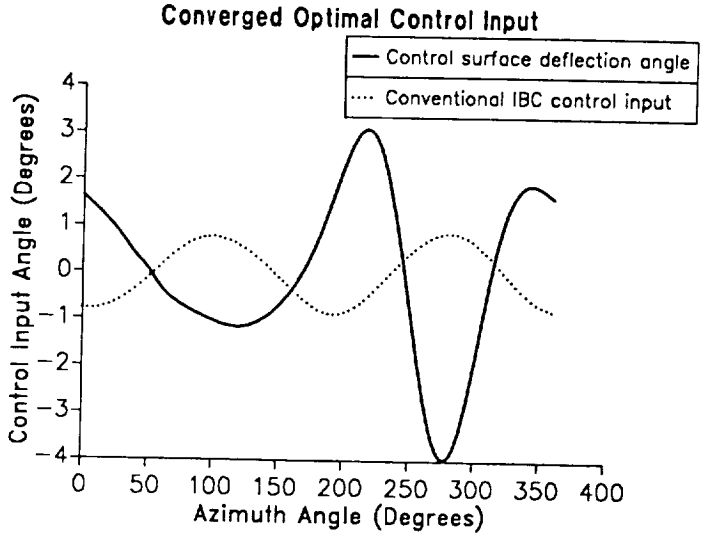

Fig. 12: Optimal control input comparison at a first rotating torsional frequency of 2.5/rev

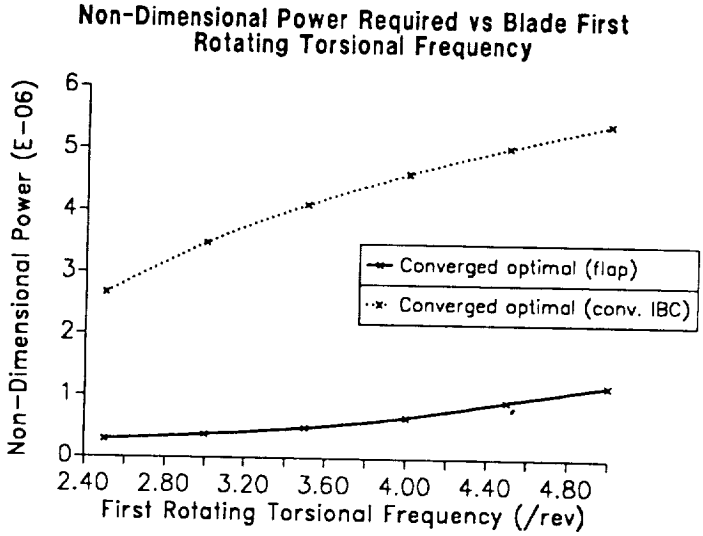

Fig. 13: Power requirements vs. blade first rotating torsional frequency